PHYSICS AND CHEMISTRY OF SOLID STATE
V. 27, No. 2 (2026) pp. 346-355
Section: Technology

DOI: 10.15330/pcss.27.2.346-355

Vasyl Stefanyk Carpathian National University

ФІЗИКА І ХІМІЯ ТВЕРДОГО ТІЛА
Т. 27, № 2 (2026) С. 346-355
Технічні науки

PACS: 44.05.+e

ISSN 1729-4428 (Print)
ISSN 2309-8589 (Online)

I.R. Vashchyshak, S.P. Vashchyshak, T.M. Mazur, M.P. Mazur

Experimental study of heat transfer in a wick heat pipe with a magnetic stainless steel wick at various inclination angles

Ivano-Frankivsk National Technical University of Oil and Gas, Ivano-Frankivsk, Ukraine, tetiana.mazur@nung.edu.ua

This paper presents the results of an experimental study into the operation of a wick-type heat pipe equipped with an innovative induction heating system. This work is a logical continuation of the theoretical studies published by the authors in 2025 and aims to verify the mathematical model of thermal processes in the 'inductor – magnetic core – heat transfer fluid' system. The design of the tube under investigation comprises a copper casing, a wick based on an AISI 304 stainless steel mesh, and a ferromagnetic core made of AISI 430 steel. Heating was carried out using a parallel resonant circuit at a frequency of 28.15 kHz.

The aim of the study was to determine the effect of the tilt angle on the thermal efficiency of the tube in the low-temperature range (18–50°C). The architecture of the experimental setup is described, which includes a dual-channel thermometer based on an Arduino microcontroller and film thermistors, which ensure high measurement accuracy in the evaporation and condensation zones.

A series of experiments yielded sets of temperature curves for tilt angles of 30°, 45°, 60° and 90°. It was found that, when oriented vertically (90°), the tube exhibits the highest isothermal behaviour and the shortest time to reach steady state. A characteristic temperature threshold for the activation of the phase transition was identified in the range of 30–32°C. It has been demonstrated that when the tilt angle is reduced below 30°, thermal efficiency decreases significantly; this is due to the limited capillary potential of the AISI 304 steel wick, which does not ensure sufficient return of condensate to the heating zone under conditions of weak gravitational influence. The data obtained allow for the optimisation of heat pipe parameters for their use in mobile personal heating systems, particularly in thermal mats, and indicate the need to modernise the wick structure for operation in a horizontal position.

Keywords: experimental setup, finned heat pipe, induction heating, angle of inclination, heat transfer, thermal efficiency.

Receive 09 April 2026; Accepted 28 May 2026; Published 27 June 2026.

Introduction

Personal body-warming systems integrated into sleeping mats and portable mattresses come in several main types. The most common are electric sleeping mats, which use flexible wire heating elements or carbon films. They provide a rapid rise in temperature and the ability to regulate the heat setting, but have limitations regarding the uniformity of heat distribution and risks of localised overheating [1, 2]. ч

In particular, research into flexible electric heating elements shows that wire heaters are characterised by localised heat generation along the conductor, which leads to temperature gradients across the surface of the product. At the same time, carbon films and composite materials based on carbon nanotubes or fibres ensure a more uniform temperature distribution due to the planar nature of conductivity; however, their efficiency depends to a large extent on the homogeneity of the structure and the quality of the contacts [3–5]. Furthermore, it has been established that at high current densities, localised overheating (hot spots) may occur due to variations in electrical resistance, which limits the longevity of such systems and necessitates the use of thermal stabilisation and control measures [6,7].

Another class consists of liquid systems, where heat is transferred by circulating heated water or antifreeze

through flexible channels inside the mat. Such systems provide a more uniform heat distribution due to the convective mechanism of heat transfer, but require pumps and additional power sources, which complicates the design and reduces its reliability in field conditions [1,3,8]. Furthermore, the presence of a liquid circuit increases the risk of leaks and complicates operation at low temperatures.

Air-based and hybrid systems are distinguished separately, in particular inflatable mattresses with integrated heating, which combine thermal insulation with active heating. Such designs reduce heat loss through an air layer, but are characterised by larger dimensions, thermal inertia and limited mechanical strength, which complicates their use in mobile and military applications [9–11].

In addition, temperature control systems based on thermoelectric elements (Peltier elements) are used, which can operate in both cooling and heating modes; however, their efficiency remains low due to the fundamental limitations of thermoelectric materials and additional losses from Joule heating, and the design is sensitive to mechanical and thermal stresses [12,13]. This limits their widespread use in portable personal heating systems.

For tourists and military personnel, the system's high reliability, durability and autonomy are particularly important, as it must operate in harsh climatic conditions, with limited energy sources and under high mechanical stress. This is precisely why the search for new technologies capable of ensuring efficient heat exchange, simplicity of design and durability is so relevant. Consequently, the use of induction-heated heat pipes, which combine high thermal efficiency, the absence of moving parts and the ability to operate in mobile personal heating systems, represents a promising avenue.

I. Problem Statement

In order to assess the adequacy of the mathematical model of a heat pipe [14] under practical conditions and to determine its thermal efficiency using induction heating via a parallel resonant circuit, it is necessary to construct an experimental setup that will enable the determination of temperature gradients along the length of the heat pipe body in the range of 18–50°C at various angles of inclination (with a resolution of 10°) and to investigate the feasibility of using a heat pipe as a component of a system for warming the human body in field conditions.

For the first time, the effectiveness of a wick-type heat pipe with induction heating in the range of 18–50°C has been experimentally confirmed, and a mathematical model of heat transfer has been verified. The temperature threshold for phase transition activation (30–32°C) and the critical angle of inclination (~30°) for an AISI 304 steel wick have been established, below which thermal efficiency drops sharply. An approach is proposed to improve it in the horizontal position by optimising the heat transfer fluid parameters and modernising the platen structure.

II. Presentation of the main material

Based on the findings of the scientific paper [14], a copper heat pipe with a ferromagnetic core was fabricated for induction heating using fixed-frequency alternating current. A stainless steel wick was selected due to its low corrosion activity. The vacuum valve and lower cap were attached to the tube body by soldering with a tin-lead alloy. The working pressure of the saturated vapour inside the evacuated heat pipe was 12.3 kPa at a temperature of 50°C. The weight of the pipe was 270 g. The properties of the materials from which the heat pipe is made are given in Table 1.

Researchers studying heat pipes have developed several experimental setups that allow the orientation of the pipes to be adjusted in space [15,16]. However, these setups are overly complex and bulky. For this study, a compact, simple-design setup is proposed, which allows the inclination of the heat pipe to be adjusted from 90° to 0°, to heat it, and to measure the temperature in its upper and lower sections.

A functional diagram of the experimental setup for investigating heat transfer in a manufactured heat pipe (without a system for adjusting its angle of inclination) is shown in Fig. 1. The tube temperature was measured by two sensors (thermistors) Rt1 and Rt2, fixed in its lower

Table 1.

Properties of the main materials used in the manufacture of the heat pipe

Part	Material	Length, mm	Diameter, mm	Wall thickness, mm	Porosity, mesh	Volume, ml	Number of coils
Tube casing	Copper	500	18	1			
Wick	AISI 304 stainless steel	450	16	0.23	100		4
Core frame	S-Glass	30	15	0.3			1
Ferro-magnetic core	AISI 430 stainless steel	26	15.6	0.3			120
Heat transfer fluid	Distilled water					4.5	
Vacuum valve	Copper	12	16	1.2			
Bottom cover	Copper	8	16	1			

(5 cm from the lower end) and upper (1 cm from the upper end) sections. Signals from the sensors were fed to the bridge measurement circuits of the 2-channel temperature measurement unit A1 with display. There, they were processed by an Arduino UNO board and displayed on the digital display of each channel, as well as transmitted to a PC via a USB port. The A1 temperature measurement unit was powered by a highly stable voltage from the UZ1 power supply.

The induction heating system for the heat pipe consists of an inductor (L) wound around the heat pipe housing and a capacitor (C) connected in parallel to it, forming an L-C resonant circuit. The circuit operates in resonance mode at a frequency of 28.15 kHz, which ensures maximum heating power of the ferromagnetic core.

The power amplifier (A2) is based on a half-bridge circuit using MOSFETs [14]. It amplifies the signal current to excite the electromagnetic field in the resonant L-C circuit.

The master oscillator (G1) generates a stable sinusoidal signal with a frequency of 28.15 kHz, which is fed to amplifier A2.

A digital oscilloscope (PS1) is connected in parallel to the L-C circuit and the output of the master oscillator to monitor resonance phenomena and the signal waveform.

Since the heat pipe is required to operate at relatively low temperatures (up to +50°C), a two-channel thermometer (Fig. 2) was developed for the experimental setup, designed for the precise measurement and visualisation of temperature at two points along the heat pipe (the evaporator and the condenser). The input stage of the thermometer U1 comprises a two-channel bridge measurement circuit based on the LM324 operational amplifier (DA1). This allows the change in resistance of the thermistors (Rt1, Rt2) to be converted into a voltage with high noise immunity. Additional stabilisation of the +5.2 V supply voltage for the measuring bridges (R1–R5 and R10–R14) is provided by the 7805 regulator (DA2).

The Atmega 328 microcontroller on the Arduino UNO board (U2) performs analogue-to-digital conversion and calculates the temperature according to the calibration curves. An indicator unit based on two TM1637 modules (U3, U4) is used to display the current temperature values for each channel separately. The microcontroller is programmed and measurement results are recorded using the U5 PC.

Miniature thermistors in a protective film sheath with heat-resistant insulation are used to measure the temperature at the tube surface; signals from these are transmitted via twisted-pair cables to reduce electromagnetic interference (Fig. 3) [17,18]. The calibration of sensors Rt1 and Rt2 was carried out by comparison with a Fluke 54 II reference thermometer [19,20] and a K-type immersion thermocouple in a water bath (Fig. 4). The resulting calibration curves were entered

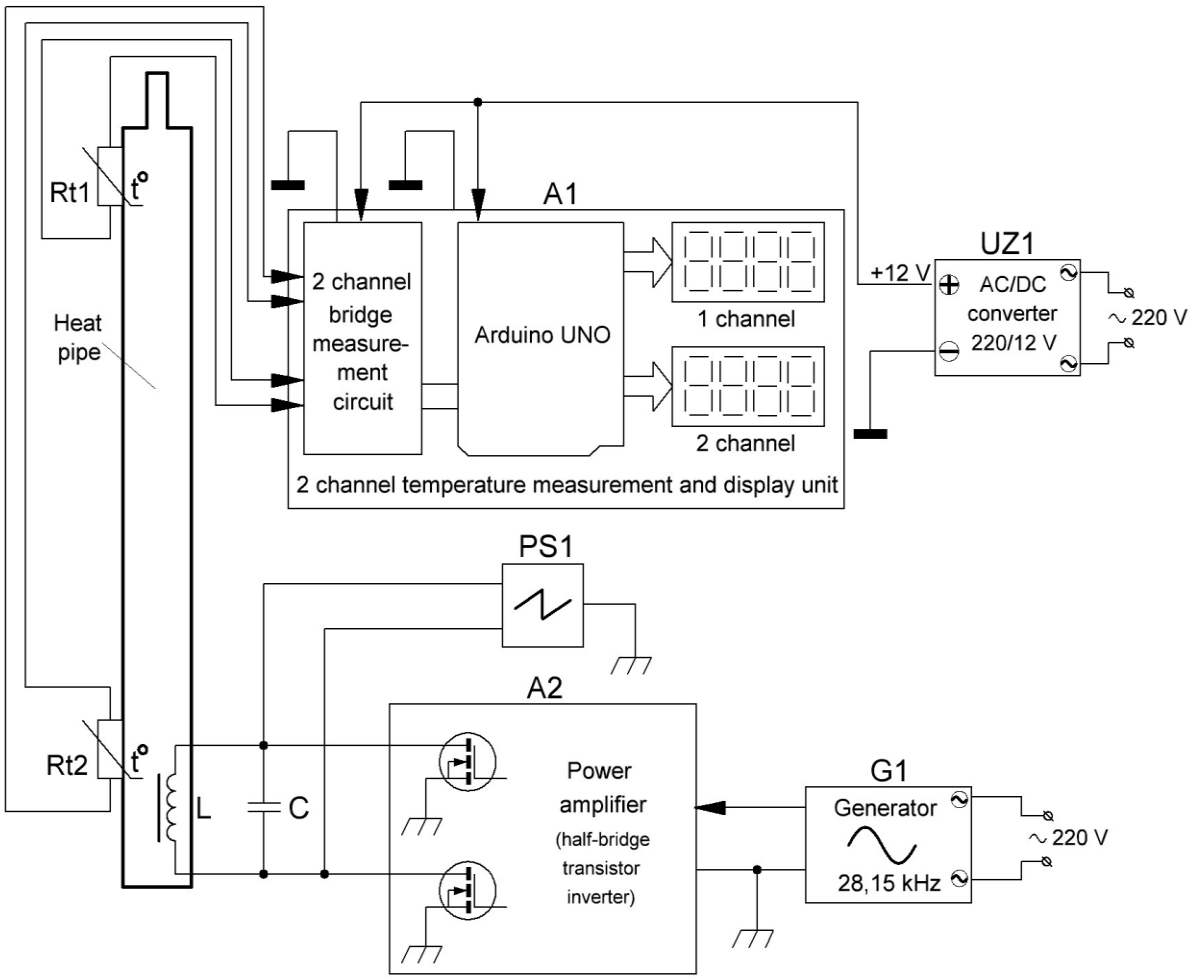

Fig. 1. Block diagram of the experimental setup for investigating heat transfer in a wick-type heat pipe.

into the microcontroller's operating program to correct the data from the thermistors.

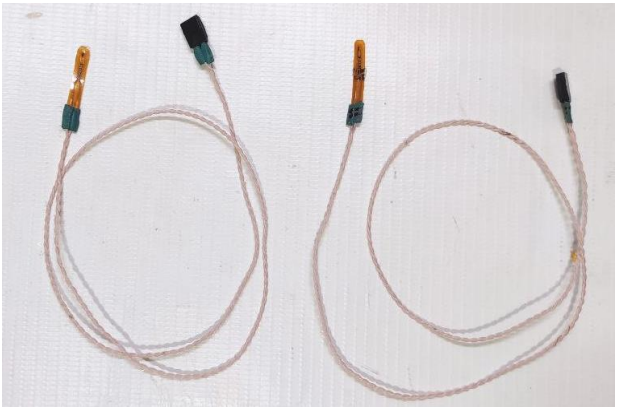

Fig. 3. Appearance of thermistors.

Fig. 4. Calibration of thermistors in a water bath.

The external appearance of the heat pipe, featuring a power amplifier enclosed in a protective casing with a mounting hole for attachment to the installation, and the temperature sensors mounted on it, is shown in Fig. 5.

Fig. 5. External view of a heat pipe with a power amplifier and temperature sensors.

To adjust the angle of inclination of the heat pipe and secure its position, a special jig has been developed, which allows the amplifier's protective casing to be attached to a swivel bracket. Precise fixing of the tube's tilt angle was achieved by resting its upper part on a fixed thermal insulation rod in accordance with the drawing on the bracket (Fig. 6). The distance from the surface of the heat pipe to the surface of the bracket, to avoid thermal shielding, was 20 mm.

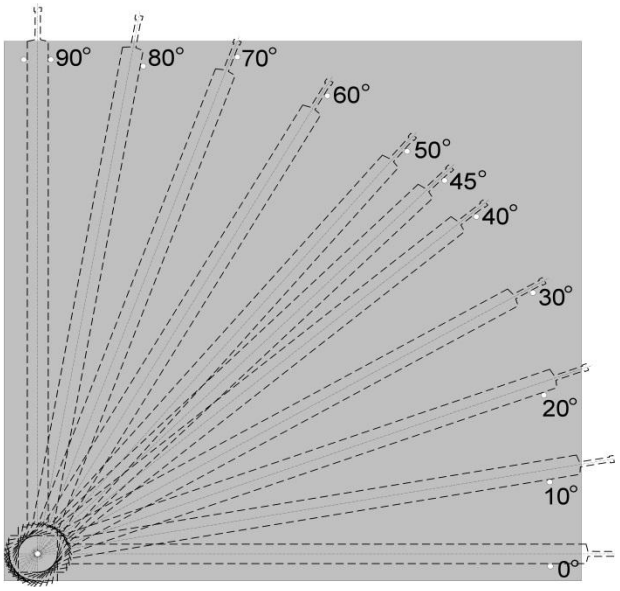

Fig. 6. Die for adjusting the orientation angle of the heat pipe.

The external view of the experimental setup with the heat pipe under investigation, the system for changing its tilt angle, a 2-channel thermometer and all necessary instruments is shown in Fig. 7.

The operating algorithm for the induction heating system of the heat pipe, designed to prevent significant internal vapour pulsations, involved a gradual increase in the electrical power of the signal supplied to the resonant L-C circuit from 1 to 10 W during the initial heating stage (up to 24 °C). To prevent heat transfer crisis, a gradual reduction in power from 10 to 3 W was envisaged during the final heating stage (above 44°C).

The use of a sinusoidal excitation signal for the resonant L-C circuit is necessitated by the need to reduce electromagnetic interference affecting the operation of the thermistors in the temperature measurement unit. When implementing the circuit for practical applications, it is advisable to use square-wave pulses and field-effect transistor switches to drive the L-C circuit. This will improve the efficiency of converting electrical pulses into heat and simplify the electrical circuit.

The initial temperatures at the lower end of the heat pipe (temperature sensor Rt2) at different angles of orientation ranged from +18.0°C to +18.6°C, and at the upper end (temperature sensor Rt1) from +19.5°C to +19.6°C. Heating of the tube ceased when the temperature in the vicinity of the condenser (Rt1) reached +50°C.

For each angle of inclination of the heat pipe, temperature curves of its heating in the lower and upper sections were obtained (Fig. 8). These curves are significantly noisy, which is explained by the influence of the oscillating L-C circuit on the temperature sensors Rt1 and Rt2, which, having a high resistance (around 10 kΩ), acted as antennas for the circuit's alternating electromagnetic field. Furthermore, the current consumption varied by up to 20% at the inductor's maximum power. Therefore, the experimental data were processed using digital filtering methods to eliminate high-frequency interference from the resonant inductor, specifically the Average function.

The experiments yielded curves showing the

temperature changes in the evaporator and condenser (in °C) as a function of time (in seconds) for all the specified angles on the die. The most representative of these are shown in Figs. 9–13. To better understand the behaviour of the heat pipe, Figs. 14 and 15 show families of temperature curves recorded in its lower and upper sections.

The experiments conducted confirm the main prediction of the model [1] that induction heating of the magnetic core is an effective method for initiating heat flow. The temperature curves (Figs. 14, 15) have a characteristic exponential shape, which coincides with the calculated model of the heat capacity of the components.

Figures 9–13 show that as the angle of inclination of the heat pipe decreases, the temperature of its upper section rises more slowly, indicating a reduction in the influence of gravitational forces on the process of fluid return through the porous wick structure. At tilt angles ranging from 90° to 60°, the tube operates in thermosiphon mode, where gravity assists the capillary forces in returning the condensate. Here, we observe the fastest transition to steady-state operation. At tilt angles of 30° and less, thermal efficiency decreases. At small tilt angles, the liquid layer is distributed unevenly, leading to partial 'drying out' of the heating zone.

In the graphs obtained, a change in the slope of the Rt1 curve (condenser) is observed within the range of 30–32°C. This indicates that the vapour pressure threshold has been exceeded and the temperature threshold for phase transition activation has been reached.

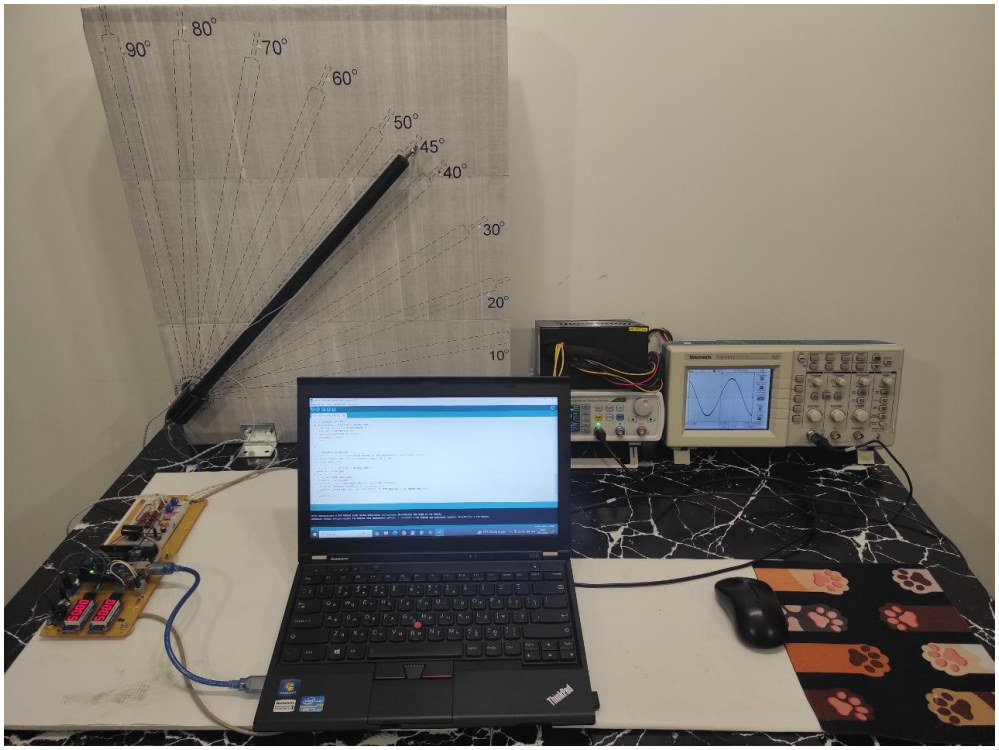

Fig. 7. External view of the experimental setup for studying the heat pipe.

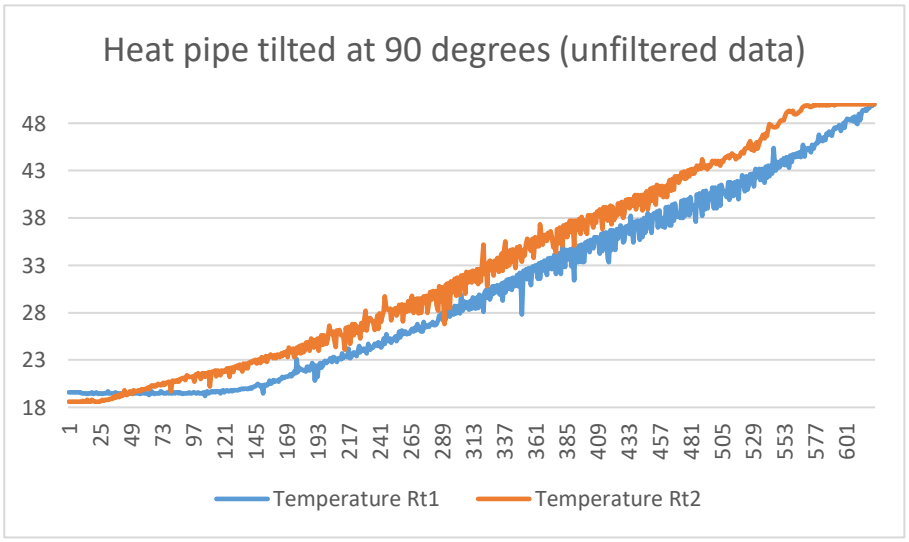

Fig. 8. Temperature curves, with noise introduced by the operation of the induction heating system for the heat pipe (vertical orientation of the pipe).

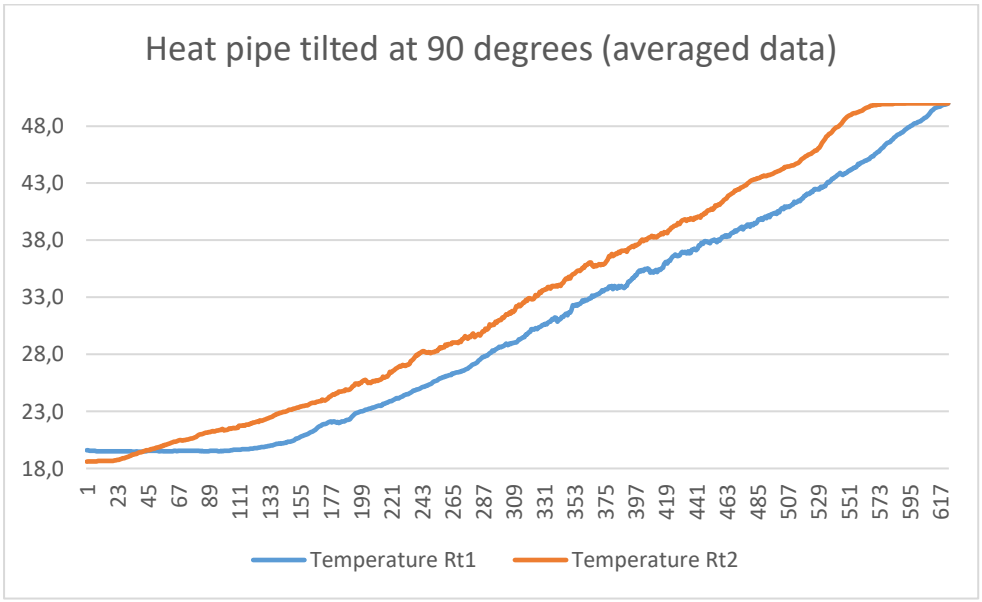

Fig. 9. Temperature curves smoothed using the Average function (tube in a vertical position).

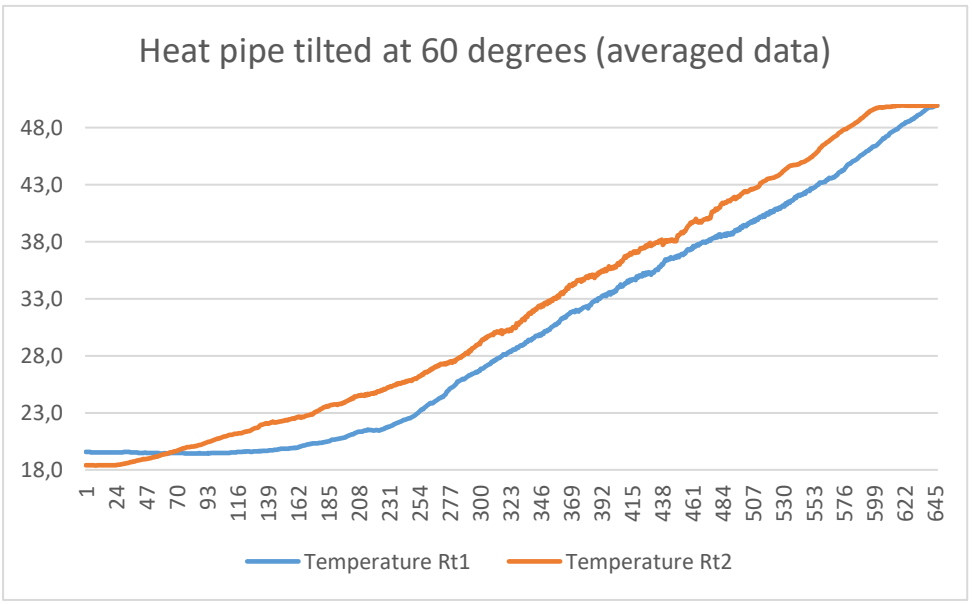

Fig. 10. Temperature curves smoothed using the Average function (tube tilt 60°).

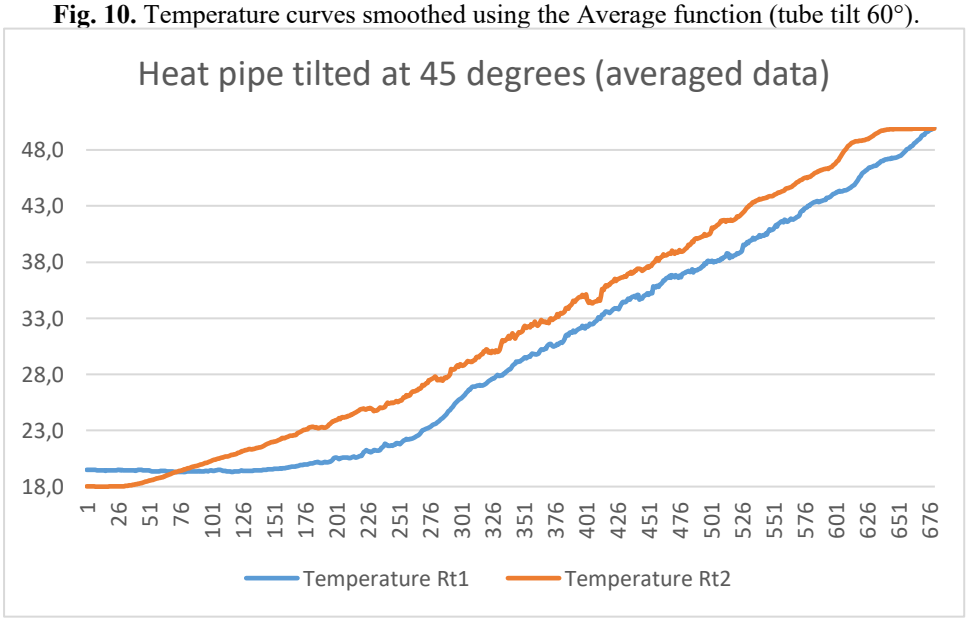

Fig. 11. Temperature curves smoothed using the Average function (tube tilted at 45°).

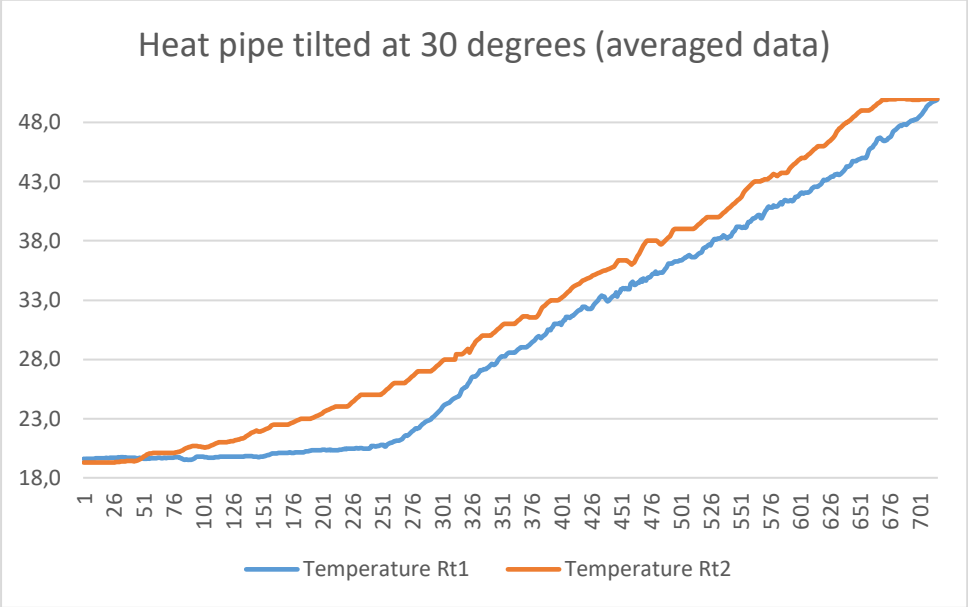

Fig. 12. Temperature curves smoothed using the Average function (tube tilt 30°)

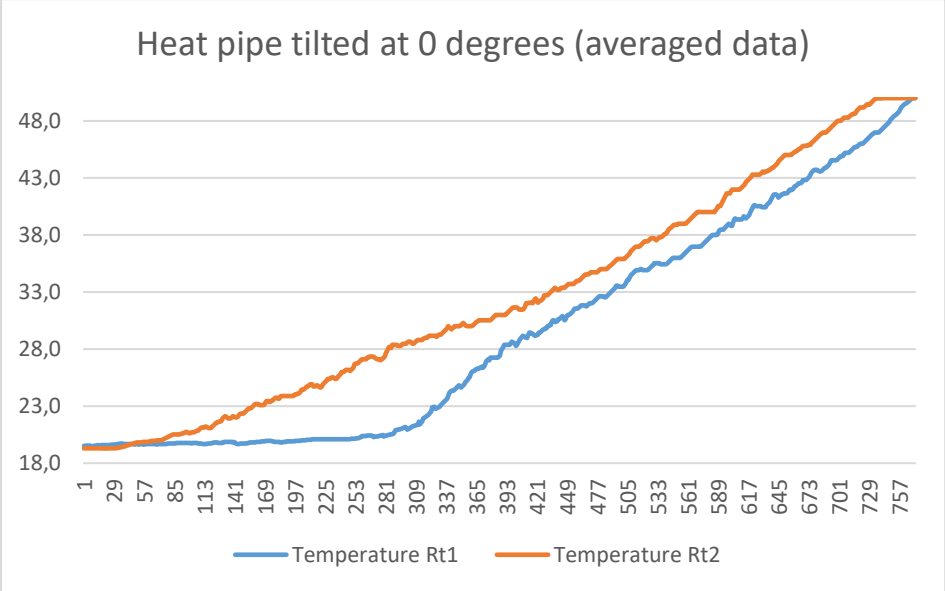

Fig. 13. Temperature curves smoothed using the Average function (tube in a horizontal position).

The presence of a copper casing explains why the Rt1 and Rt2 curves in Fig. 9 (90°) converge so closely. Copper instantly equalises the temperature. However, at 30° (Fig. 12), the gap widens. This happens because the liquid 'runs' to the bottom of the tube, and the steel wick does not have time to distribute it around the entire perimeter of the copper wall. Experiments have shown that even with an ideal copper casing, the angle of inclination remains a critical factor. This confirms that the weak link is indeed the AISI 304 steel wick. Since steel is less wettable by water than copper, the capillary potential of the wick mesh is limited. The experiment also shows a greater temperature gradient between the evaporator and the condenser than predicted by the idealised model. This is explained by the contact thermal resistance between the magnetic core and the inner wall of the tube, as well as the thermal resistance of the steel wick housing (AISI 304), which has a much lower thermal conductivity than copper.

The data obtained for the temperatures in the evaporation and condensation zones (Figs. 14 and 15) show that, with the power consumption of the tube induction heating system at around 10 W, the time taken to reach steady state was: at 90° – 300 s, at 60° – 330 s, at 45° – 342 s, at 30° – 388 s, at 0° – 422 s. The condensation zone reached its maximum temperature: at 90° in 622 s, at 60° in 646 s, at 45° in 680 s, at 30° in 718 s, at 0° in 774 s. The greatest temperature difference between the evaporator and the condenser was: at 90° – 2.7°C, at 60° – 3.3°C, at 45° – 4.0°C, at 30° – 4.8°C, at 0° – 7.8°C.

From an analysis of the families of curves in Figs. 14 and 15, it can be said that in practice the heat pipe will operate in a horizontal position (unlike the model), but its thermal efficiency will be much lower than in positions close to vertical. This limits its application as a component of a system for individual body heating, for example in thermal mats, where inclinations close to horizontal are required. To increase the thermal efficiency of the tube in

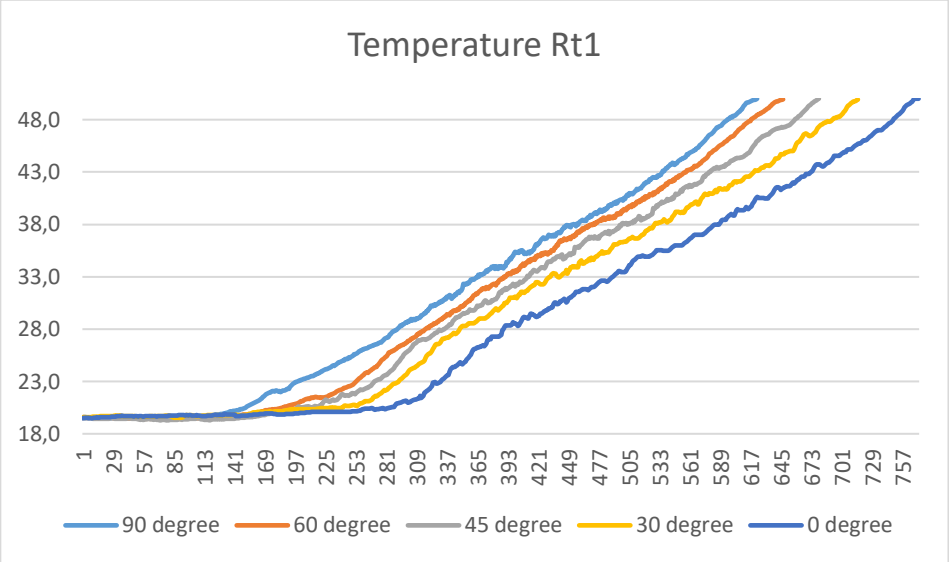

Fig. 14. A set of temperature curves recorded in the upper part of the heat pipe (condensation zone) at different angles of inclination.

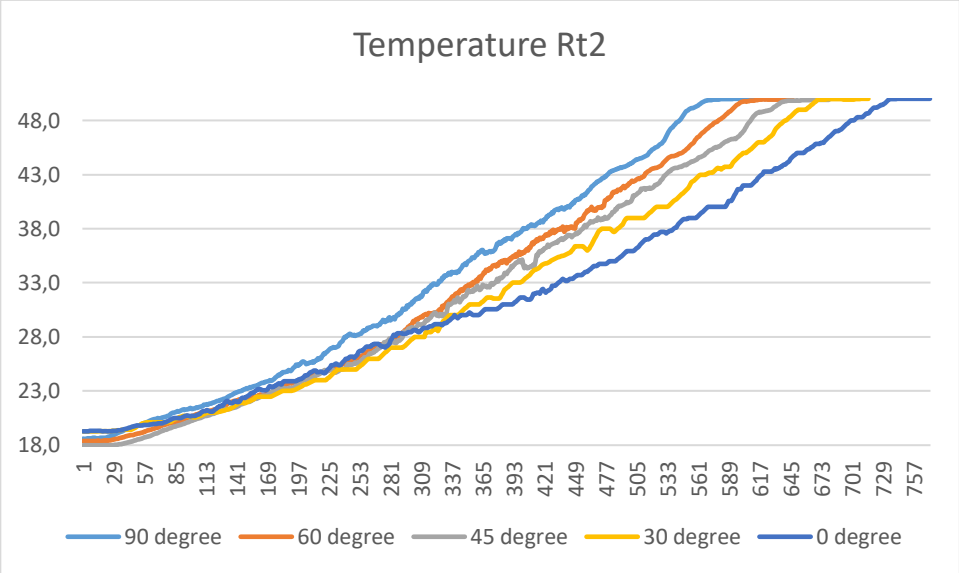

Fig. 15. A set of temperature curves recorded in the lower part of the heat pipe (evaporation zone) at different angles of inclination.

positions close to horizontal, in our opinion, the following should be done:

– degas the working fluid (distilled water) to eliminate 'thermal plugs' – areas where vapour cannot circulate freely – and to reduce the chemical activity of the medium, which contributes to copper corrosion;

– top up the tube with 10–15% working fluid to increase its volume in the horizontally positioned wick, which will reduce drying out;

– replace the wick mesh material from AISI 304 stainless steel with copper to increase capillary pressure due to the oxide film, reduce the contact angle, and increase thermal conductivity by several orders of magnitude.

A copper wick has much lower corrosion resistance than one made of stainless steel; however, as the environment will consist of degassed distilled water and a vacuum, and the maximum temperature is quite low, the corrosion process will be very slow. However, a copper wick will have low thermal resistance and a strong capillary effect, which will significantly increase the thermal efficiency of the tube in positions close to horizontal.

A sintered powder wick will have an even higher capillary effect due to the heterogeneity of its structure; however, its manufacture is costly.

Conclusions

Experimental studies have confirmed the accuracy of the mathematical model of a heat pipe with induction heating of the magnetic core; the error between the theoretical and experimental values of the steady-state temperature did not exceed 12%. It has been established that intensive heat exchange begins when the evaporator temperature reaches 30–32°C, which corresponds to the initial phase of active vapour formation.

A significant influence of the gravitational component on thermal efficiency has been identified: the best isothermal performance was achieved at tilt angles of 60–90°, where the tube operates in thermosiphon mode, ensuring rapid transition to steady state (300–330 s) and a minimum temperature difference (2.7–3.3°C). When the tilt angle is reduced to 30° or less, efficiency drops sharply, the time to reach steady state increases to 388–422 s, and the temperature difference reaches 4.8–7.8°C, which is due to the insufficient capillary potential of the AISI 304 steel mesh. This confirms that the weak link in the design is the steel wick itself, which has high thermal resistance and low water wettability.

To improve the efficiency of the tube in positions close to horizontal, it is recommended to degas the working fluid to eliminate thermal plugs, top up the tube with an additional 10–15% of water to reduce wick drying, and replace the steel mesh with a copper one, which will ensure a strong capillary effect and low thermal resistance.

The design of a heat pipe with a copper casing and induction heating of the core is promising for use in thermal mattresses; however, for stable operation in a horizontal position, modernisation of the wick structure (copper mesh or sintered powders) is required, which will significantly improve thermal efficiency.

Authors' contributions.

I.R. Vashchyshak: concept development, methodology, validity testing, writing, peer review, and editing.

S.P. Vashchyshak: conceptualization, methodology, validation, writing, peer review, and editing.

T.M. Mazur: research, writing, reviewing, and editing; project administration.

M.P. Mazur: writing, reviewing, and editing; manuscript submission.

Acknowledgments.

T.M. Mazur's research was funded by the National Foundation for Scientific Research of Ukraine (project 2025.07/0427 "Modern comprehensive probabilistic methods for studying the asymptotic properties of analytical solutions to differential equations represented by multiple random series and integrals, and their potential applications," 0126U002547).

Vashchyshak I.R. – Candidate of Technical Sciences, Associate Professor, Department of Energy Management and Technical Diagnostics;
Vashchyshak S.P. – Candidate of Technical Sciences, Associate Professor, Head of the Department of Information Technologies;
Mazur T.M. – Doctor of Philosophy, Associate Professor of the Department of Physical and Mathematical Sciences;
Mazur M.P. – Candidate of Physical and Mathematical Sciences, Associate Professor, Director of the Institute of Architecture, Construction, and Energy.

[1] Shu Fang, Rui Wang, Haisu Ni, Hao Liu, Li Liu, *A review of flexible electric heating element and electric heating garments*, Journal of Industrial Textiles, 51, (2022); https://doi.org/10.1177/1528083720968278.
[2] Song-Lin Jia, Hong-Zhang Geng, Luda Wang, Ying Tian, *Carbon nanotube-based flexible electrothermal film heaters with a high heating rate*, Royal Society Open Science, 5(6), (2018); https://doi.org/10.1098/rsos.172072.
[3] Zhu Zhu, Hao Lu, Wenjun Zhao, Ailidaer Tuerxunjiang, Xiqiang Chang, *Materials, performances and applications of electric heating films*, Renewable and Sustainable Energy Reviews, 184, 113540 (2023); https://doi.org/10.1016/j.rser.2023.113540.
[4] Taejin Kim, Deborah Chung, *Carbon fiber mats as resistive heating elements*, Carbon, 41(12), 2436 (2003); https://doi.org/10.1016/S0008-6223(03)00288-4.
[5] Ya M. Kusyi, O. R. Onysko, A. M. Kuk, O. S. Kostiuk, B. V. Solohub, *Development of the structure and methodological support of the system for analysis of the details shaping*, IOP Conference Series: Materials Science and Engineering, 2540(1), 012026 (2023); https://doi.org/10.1088/1742-6596/2540/1/012026.
[6] Dezhao Li, Yangtao Ruan, Chuangang Chen, Wenfeng He, Cheng Chi, Qiang Lin, Design and Thermal Analysis of Flexible Microheaters, Micromachines, 13(7), 1037 (2022); https://doi.org/10.3390/mi13071037.
[7] Qingshuai Yan et al., *Flexible, high-strength, and breathable electric heater with 3D folding structure for personal thermal management*, Materials Today Energy, 54, 102074 (2025); https://doi.org/10.1016/j.mtener.2025.102074.
[8] Jeong Eun Yoon, Jiwon Chung, Jeongpyo Lee, Seung Hyun Jee, Sumin Helen Koo, *Development and evaluation of cable-less heating mats utilizing low-power carbon nanotube planar heaters*, Textile Research Journal, 95(7–8), 2024; https://doi.org/10.1177/00405175241286545.
[9] ASTM International, Standard Guide for Selection of Materials for Thermal Insulation, ASTM C1055 (2019).
[10] F.P. Incropera, D.P. DeWitt, T.L. Bergman, A.S. Lavine, *Fundamentals of Heat and Mass Transfer*, 7th ed. (Wiley, Hoboken, 2011).
[11] Y. Li, A.S.W. Wong, Clothing Biosensory Engineering (Woodhead Publishing, Cambridge, 2006).
[12] I.R. Vashchyshak, S.P. Vashchyshak, T.M. Mazur, M.P. Mazur, *Study of the influence of the environment on the efficiency of induction heating of low-temperature heat pipe*, Physics and Chemistry of Solid State, 25(4), 784–794 (2024); https://doi.org/10.15330/pcss.25.4.784-794.
[13] The effects of bed cooling on sleep quality and sleep thermal comfort in overheated bedrooms, Building and Environment (2026); https://doi.org/10.1016/j.buildenv.2026.114213.
[14] I.R. Vashchyshak, S.P. Vashchyshak, T.M. Mazur, M.P. Mazur, *Study of the heat transfer efficiency of a wick heat pipe with induction heating*, Physics and Chemistry of Solid State, 26(3), 613 (2025); https://doi.org/10.15330/pcss.26.3.613-621.

[15] Huanfa Wang, Guiping Li, Xiaobin Shen, Yong Liu, Yuandong Guo, *Experimental Study and Visual Observation of a Loop Heat Pipe*, Energies, 16(13), 5068 (2023); https://doi.org/10.3390/en16135068.
[16] Deepak Dubey et al., Experimental & Theoretical Analysis of Heat Pipe at Different Orientation, IJSRD, 6(2), (2018); https://www.ijsrd.com/articles/IJSRDV6I20699.pdf.
[17] R. Pallás-Areny, J.G. Webster, *Sensors and Signal Conditioning*, 2nd ed. (John Wiley & Sons, New York, 2001).
[18] J.P. Bentley, Principles of Measurement Systems, 4th ed. (Pearson Education, Harlow, 2005).
[19] Fluke Corporation, Fluke 54 II B Digital Thermometer – Technical Data (Everett, WA, 2020).
[20] NIST, Calibration of Temperature Sensors in Liquid Baths (Gaithersburg, 2019).

І.Р. Ващишак, С.П. Ващишак, Т.М. Мазур, М.П. Мазур

Експериментальне дослідження теплопередачі гнітової теплової трубки з оседям з магнітної нержавіючої сталі при різних кутах її нахилу

Івано Франківський національний технічний університет нафти і газу, м. Івано-Франківськ, Україна,
tetiana.mazur@nung.edu.ua

Представлено результати експериментального дослідження функціонування гнітової теплової трубки з інноваційною системою індукційного нагріву. Робота є логічним продовженням теоретичних досліджень, опублікованих авторами у 2025 році, та спрямована на верифікацію математичної моделі теплових процесів у системі «індуктор – магнітне осердя – теплоносій». Конструкція досліджуваної трубки включає мідний корпус, гніт на основі сітки з нержавіючої сталі AISI 304 та феромагнітне осердя зі сталі AISI 430. Нагрівання здійснювалося за допомогою паралельного резонансного контуру на частоті 28,15 кГц.

Метою роботи було визначення впливу кута нахилу на теплову ефективність трубки в низькотемпературному діапазоні (18–50°C). Описано архітектуру експериментальної установки, що включає двоканальний термометр на базі мікроконтролера Arduino та плівкових терморезисторів, які забезпечують високу точність вимірювань у зонах випаровування та конденсації.

В результаті серії експериментів отримано сімейства температурних кривих для кутів нахилу 30°, 45°, 60° та 90°. Встановлено, що при вертикальній орієнтації (90°) трубка демонструє найвищу ізотермічність та мінімальний час виходу на стаціонарний режим. Виявлено характерний температурний поріг активації фазового переходу в районі 30–32°C. Доведено, що при зменшенні кута нахилу нижче 30° теплова ефективність суттєво знижується, що зумовлено обмеженим капілярним потенціалом сталевого гніта AISI 304, який не забезпечує достатнього повернення конденсату в зону нагріву в умовах слабкого впливу гравітаційної складової. Отримані дані дозволяють оптимізувати параметри теплових трубок для їх застосування в мобільних системах індивідуального обігріву, зокрема в термокарематах, та вказують на необхідність модернізації гнітової структури для роботи в горизонтальному положенні.

Ключові слова: експериментальна установка, гнітова теплова трубка, індукційний нагрів, кут нахилу, теплопередача, теплова ефективність.